Astron. Astrophys. 281, 673–680 (1994)

ASTRONOMY AND ASTROPHYSICS

Sensitive limits on the molecular gas content of cluster cooling flows

B.R. McNamara[1,2,⋆] **and W. Jaffe**[3,⋆]

[1] Kapteyn Astronomical Institute, Postbus 800, NL-9700AV, Groningen, The Netherlands
[2] Harvard-Smithsonian Center for Astrophysics, 60 Garden St. MS-6, Cambridge, MA 02138, USA
[3] Sterrewacht Leiden, P.O. Box 9504, NL-2300RA, Leiden, The Netherlands

Received December 9, 1992; accepted June 2, 1993

Abstract. We have searched for molecular gas toward six cluster cooling flows in the CO(2–1) line using the James Clerk Maxwell Telescope. The sample includes clusters with estimated total cooling rates of $\dot{m}_{\rm CF} \sim 10$–$600 M_\odot$ yr^{-1}, at redshifts between $z \sim 0.01$–0.06. None were detected either in emission or absorption. Our molecular mass limits in the inner ~ 25 kpc are typically $M_{\rm H_2} \lesssim 4\,10^9 M_\odot$. Our limit for the nearest cluster, A 1060, is an order of magnitude lower. In the aggregate, these are the most sensitive limits available for cluster cooling flows. Using model spectra we find that molecular cloud populations as massive as few $10^{10} M_\odot$ with velocity dispersions $\lesssim 500$ km s^{-1} are usually excluded, unless the material is colder and/or and has a significantly lower metal abundance compared to average Galactic clouds. If the steady state cooling flow model is correct, the cooling material must be converted efficiently to a non-gaseous state on a timescale of $\sim 10^{7-8}$ yr, or the putative cold clouds must be accelerated to a velocity dispersion $\gtrsim 700$ km s^{-1} on a similar timescale. Future observations with broader bandwidths should yield improved limits. Failure to detect CO at levels significantly lower than these may be difficult to reconcile with standard cooling flow models.

Key words: galaxies: clustering – galaxies: ISM – intergalactic medium – radio lines: galaxies – X-rays: galaxies – galaxies: cooling flows

1. Introduction

X-ray observations of clusters of galaxies have shown that a large fraction of the total mass of clusters is present as a hot ($\sim 10^{7-8}$ K), diffuse ($n_0 \sim 10^{-3}$ cm^{-3}) plasma (see Forman & Jones 1982; Sarazin 1986 for reviews). In many clusters the gas densities in the central 100–200 kpc are high enough ($n_0 \gtrsim 10^{-1}$ cm^{-3}) that the radiative cooling time becomes shorter than the Hubble time. In the absence of heating, the gas is inferred to be cooling at rates of $\sim 100 M_\odot$ yr^{-1} (see Fabian 1988, 1991 for reviews). This would result in $\sim 10^{12} M_\odot$ of accumulated material if the cooling occurred steadily at these rates over the Hubble time. The final state of most of the cooling material (e.g. stars or cold gas) in "cooling flow" clusters has yet to be identified. However, some fraction of the putatively cooling material should reside in cool (10–100 K) atomic and/or molecular clouds.

Early searches for the 21 cm emission line of atomic hydrogen in clusters revealed only upper limits of $\sim 10^{9-10} M_\odot$ (Burns et al. 1981; Valentijn & Giovanelli 1982). Later searches have lead to the detection of H I in absorption in four clusters with large cooling flows and improved emission upper limits of $\sim 10^{8-9} M_\odot$ [see Jaffe (1992) for a review]. The absorption features have column densities of $N_{\rm H\,I} \sim 10^{18-20}$ (T_s/100 K), and velocity widths of 30–500 km s^{-1}. These limits have largely excluded H I as a plausible repository for the cooling material.

Previous searches for molecular gas (i.e. CO) in more than a dozen clusters with cooling flows have resulted in one detection, NGC 1275 (Lazareff et al. 1989; Mirabel et al. 1989), but otherwise typical H_2 upper limits of $\sim 10^{10} M_\odot$ (Bregman & Hogg 1988; Grabelski & Ulmer 1990). Although, the kinematics of the CO in NGC 1275 appears consistent with a cooling-flow origin (cf. Lazareff et al. 1989), the H_2 mass estimates ($\sim 10^{10} M_\odot$) cannot account for the material inferred to have been accreted over the cluster's lifetime. The limits on many remaining clusters are insufficient to exclude CO in the amount found in NGC 1275.

Due to the generally unrestrictive CO limits and the more sensitive receivers now available, a renewed search seemed appropriate. The recent H I detections and X-ray spectral anomalies attributed to absorption by cold clouds in clusters warrant additional constraints. Here we present sensitive CO(2–1) spectra for six clusters obtained with the

Send offprint requests to: B.R. McNamara
⋆ Visiting Astronomer, James Clerk Maxwell Telescope, Mauna Kea, Hawaii.

Table 1. Cluster properties

Cluster	RC	RA (1950)	Dec.[a] (1950)	z[b]	$\dot{M}$ ($M_\odot$ yr^{-1})	R_c (kpc)	$\dot{M}(d)$ ($M_\odot$ yr^{-1})
Hydra A	3C 218	09 15 41.2	− 11 53 04.9	0.0538	600	160	88
A 1060	—	10 34 21.5	− 27 16 06.6	0.0128	11	94	0.71
NGC 3311							
MKW 3s	3C 318.1	15 19 25.3	+ 07 53 13	0.0443	151	210	14
NGC 5920							
A 2151	—	16 02 20.8	+ 17 51 25	0.0348	116	160	11
NGC 6041							
A 2256	—	17 07 17.7	+ 78 42 18	0.0594	0–200[c]	—	—
Cygnus A	3C 405	19 57 44.4	+ 40 35 46.4	0.0566	187	184	26
Perseus	3C 84	—	—	0.0186	400	193	36

[a] Positions taken from: Baum et al. (1988), Vasterberg et al. (1991); McNamara et al. (1990); Dressler & Shectman (1988); Vestergaard & Barthel (1992).
[b] Redshifts taken from: Simkin (1979); McNamara & O'Connell (1989); Dressler & Shectman (1988); Osterbrock & Miller (1975); Fabricant et al. (1989); Bothun & Schombert (1990).
[c] Cooling rate from White et al. (1991) has large uncertainty.

James Clerk Maxwell 15-m Telescope. CO was not detected in any cluster. Comparing our observations to predictions of a simple, steady state cooling flow model and to model spectra, we constrain the properties of putative molecular cloud populations.

All distance- and time-dependent quantities in this paper assume $H_o = 50$ km s^{-1} Mpc^{-1}, and $q_0 = 0$.

2. Observations

2.1. Sample selection

The objects were selected primarily on the basis of having large cooling rates as estimated from X-ray observations. Other criteria were detected H I (e.g. MKW 3s), blue central colors (e.g. Hydra A-Smith & Heckman 1989; A 1060-McNamara & O'Connell 1992), a reasonably small and well determined systemic velocity, or otherwise lacking previous CO measurements.

The sample is listed in Table 1. Columns 1 and 2 list the cluster name and radio source designation. Columns 3 and 4 list the telescope pointing. In all cases these coordinates refer to the position of the centrally dominant cluster galaxy. The redshifts and positions were taken from references listed in Table 1. Due to the limited bandwidth of the receiving system, we included objects which had radial velocity errors which were quoted $\lesssim 100$ km s^{-1}. The receiver was tuned to frequencies corresponding to the redshifted frequency of the CO(2–1) line using the formula: $\nu = \nu_0/(1+z)$, where z was taken from column 5 and $\nu_0 = 230.538$ GHz is the feature's rest transition frequency. In Column 6 we list the total cooling rates of the hot intracluster medium (ICM), based largely on X-ray imaging from the *Einstein* satellite taken from either Arnaud (1988), David et al. (1990), White et al. (1991), or White & Sarazin (1987). Column 7 lists the radius within which the ICM appears to be cooling, or the "cooling radius" (cf. Sect. 3.2). Column 8 lists the cooling rate within the beam of our telescope, determined using a simple cooling-flow model which assumes $\dot{m}_{CF} \propto R$ (cf. Sect. 3.2).

2.2. JCMT observations

The CO(2–1) observations were obtained over eight nights during 1992, June, using the 15 m James Clerk Maxwell Telescope (JCMT) on Mauna Kea, Hawaii. We used the new A2 receiver with a single channel lead–alloy SIS mixer, which provided a receiver temperature of $T_{rec} \sim$ 130 K. The system temperature was $T_{sys} \sim 400$–500 K during transparent weather conditions. The receiver is tunable over frequencies 210–280 GHz. Our objects lie in the range of 218–228 GHz. The backend consisted of an acousto-optical spectrometer with a 500 MHz bandwidth and 2048 channels (250 KHz in width), corresponding to a velocity bandwidth of ~ 680 km s^{-1} and a channel width of ~ 0.4 km s^{-1} at typical frequencies. The beam full width at half maximum (FWHM) is about 21″.

The observations were done in beam-switch mode, which nutates the secondary reflector between the pointing position and an off position, located 150″ away in azimuth, with a frequency of 1 Hz. Although a larger throw would have been desirable (see Sect. 3.2), this appears to be the maximum which provides stable baselines. Antenna temperatures (T_A) were derived by observing an internal cold source every hour to two hours, depending on the weather conditions. The pointing was determined by observing Jupiter or a bright quasar every 1.5–2 h; the pointing was stable to 2″–3″. All objects were observed on multiple nights; the receiver was offset from the nominal velocity by a few MHz each night to ensure that the

Table 2. Molecular gas limits

Cluster	Int. time (min)	$T(B)^{a,b}$ (mK)	RMS[b] (mK)	V_{ch} (km s^{-1})	τ^b	$I(co)^b$ K km s^{-1}	d (kpc)	$M(H_2)^c$ ($10^9 M_\odot$)	t_a (10^8 yr)
Hydra A	155	17	18.0	0.340	< 1.43	< 0.545	30	< 3.7	< 0.4
A 1060	145	< 2	32.3	0.327	—	< 0.960	7.7	< 0.4	< 6
MKW 3s	205	< 2	13.9	0.337	—	< 0.419	25	< 2.0	< 1
A 2151	145	33	20.3	0.334	< 1.06	< 0.610	20	< 1.9	< 1
A 2256	75	< 2	30.9	0.342	—	< 0.939	33	< 7.8	—
Cygnus A	70	164	32.6	0.341	< 0.47	< 0.989	32	< 7.7	< 3
Perseus[d] NGC 1275	—	—	—	—	—	15	11	10	6

[a] Errors on the continuum level are ~ 50–100% based on night-to-night repeatability. Systematic errors could be larger.
[b] Assumes a main beam efficiency of 0.7.
[c] Limits assume a full velocity width at zero intensity of 300 km s^{-1}, comparable to what is observed in NGC 1275.
[d] Based on observations of Mirabel et al. (1989) & Lazareff et al. (1989), adjusted to a Hubble constant of 50 km s^{-1} Mpc^{-1}.

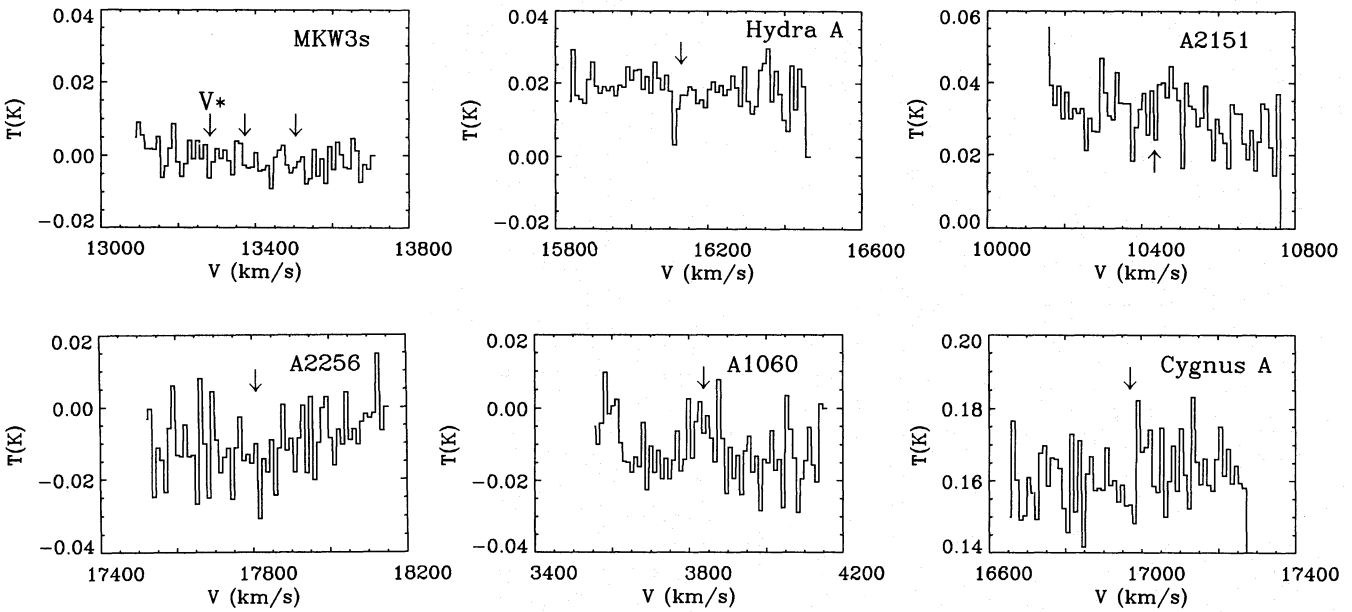

Fig. 1. CO(2–1) spectra which have been binned by 30 channels (~ 10 km s^{-1}) and corrected to T_{mb} (cf. Sect. 2.3). Baselines have not been removed. The arrows over the MKW 3s spectrum indicate the mean stellar velocity of NGC 5920 (labeled "V*") and the velocities where H I was detected in absorption (McNamara et al. 1990; Jaffe 1992) see text Sect. 3.1. The arrows in the remaining panels indicate the systemic stellar velocities of the central galaxies. No significant CO emission or absorption features are seen. The absorption feature close to the systemic velocity of Hydra A is present at only the 2σ level

spectrum fell on different channels of the receiver bank. Weather conditions were variable: two nights were lost to clouds, four nights had excellent transparency (T_{sys} ~ 390–450 K), and two nights were fair (T_{sys} ~ 700–1100 K).

2.3. Data reduction and analysis

The individual spectra consist of 300 s scans, where half of the integration time is spent on the "off" position. The longest integration was on MKW 3s, for which we obtained 41 × 300 s scans. The scans were weighted inversely by the system temperature and added to obtain the final spectrum. We obtained typically 27 individual scans for each object. The spectra were combined using the SPECX software, written by Padman. Main beam temperatures were derived as: $T_{mb} = T_A/\varepsilon$, where the main beam efficiency $\varepsilon = 0.7$. All temperature-dependent quantities in Table 2 and spectra presented in Fig. 1 have been corrected by ε.

In Fig. 1 we present the CO(2–1) spectra which have been binned by 30 channels (~ 10 km s^{-1}), converted to T_{mb}, but have had no baseline removed. The spectra show no significant CO(2–1) features either in emission or in absorption, although there is a ~2σ absorption feature close to the systemic velocity of Hydra A And a 2σ

emission feature in A1060. We estimated emission upper limits by measuring the RMS noise in the spectra following the subtraction of either a linear or second order polynomial baseline. The channels on either end of the spectrum and interference spikes were avoided. The lowest RMS noise per unsmoothed channel was 13.9 mK for MKW 3s; typical values are 25 mK. The arrows above the MKW 3s spectrum in Fig. 1 indicate the locations of earlier detections of H I in absorption (right two arrows) and the systemic stellar velocity of the centrally dominant galaxy (left-most arrow), discussed in Sect. 3.1. The arrows in the remaining panels indicate the systemic velocity of the central galaxy.

To obtain 3σ emission limits we estimated the CO brightness temperatures integrated over the line profiles using:

$$I_{\rm CO}=\frac{3\sigma_{\rm ch}\Delta V}{\sqrt{\Delta V/\Delta V_{\rm ch}}}\ {\rm K\ km\,s^{-1}}.$$

Here, $\sigma_{\rm ch}$ is the RMS deviation per unsmoothed channel after baseline subtraction, $\Delta V_{\rm ch}$ is the velocity width of each channel, ΔV is the assumed velocity full width for a rectangular emission feature. The molecular mass is often estimated using: $M_{\rm H_2}=5.82\ 10^6 I_{\rm CO(1-0)}(\pi/4)d^2$, where d is the telescope beam diameter, in kiloparsecs, at the distance of the source. The numerical factor, which converts CO intensity to H_2 column density, was taken from Sanders et al. 1984. However, this coefficient applies to the CO(1–0) line feature which is often stronger than the corresponding CO(2–1) feature. Our upper limits were estimated by multiplying this factor by the ratio of the integrated brightness temperatures in the CO(1–0) and CO(2–1) lines observed in NGC 1275 (Lazareff et al. 1989). The expression, $M_{\rm H_2}=9.7\ 10^6 I_{\rm CO(2-1)}(\pi/4)d^2 M_\odot$ has been applied in Table 2.

The results are presented in Table 2. Column 2 lists the total (on + off) integration time. Column 3 lists the mean baseline brightness temperature. The errors based on repeatability from night to night are between 50–100%. The largest departures occurred on nights of marginal weather conditions, which elevated the system temperatures. Column 4 lists $\sigma_{\rm ch}$ for unsmoothed channels, after baseline subtraction, in units of mili-Kelvins. Column 5 lists the channel width in km s^{-1} at the redshift given in Table 1. Column 6 lists upper limits for a one channel wide absorption feature estimated using: $\tau=\ln[1+3\sigma_{\rm ch}/T(B)]$. These estimates are not restrictive due to weak continuum levels. Column 7 lists the upper limit on the integrated brightness temperature for a 300 km s^{-1} full width at zero intensity rectangular line feature, $I_{\rm CO}$, in K km s^{-1}. Column 8 lists the projected metric telescope beam diameter for a 21″ beam. Column 9 lists the H_2 upper limit using $I_{\rm CO}$ from Column 7. Column 10 lists the accumulation timescale, computed as $t_{\rm a}=M({\rm H_2})/\dot{m}_{\rm CF}(d)$, discussed in Sect. 3.2.

3. Discussion

We presented limits on the integrated CO(2–1) brightness temperatures of six centrally dominant cluster galaxies centered in large cooling flows. The estimated limits integrated over velocities $\lesssim$300 km s^{-1} and galactic diameters of $\sim$25 kpc are typically $M_{\rm H_2}\lesssim 4\ 10^9 M_\odot$. For the inner 8 kpc of NGC 3311 in the nearest cluster A 1060, this limit is an order of magnitude lower. As a sample, these are the most sensitive limits available. The only cluster cooling flow galaxy in which CO has been detected, NGC 1275 in the Perseus cluster, appears to have a total cooling rate of $\dot{m}_{\rm CF}\sim 400 M_\odot\ {\rm yr}^{-1}$ (White & Sarazin 1988). There, $\sim 10^{10} M_\odot$ of molecular gas was detected (Lazareff et al. 1989; Mirabel et al. 1989). Molecular gas with similar properties would have been detected in these objects. In the next three sections, we review the evidence for cool gas in a number of our objects, and compare their CO spectra to a simple cooling flow model and to model spectra.

3.1. *Signatures of cool gas*

In addition to having X-ray signatures of cooling flows, a number of objects in our sample have optical and radio properties which indicate the presence of cool gas. They include anomalously blue central colors, optical dust features, H I absorption features, and in one case, CO in emission. These properties are briefly summarized here, and are discussed in the context of our CO observations.

MKW 3s was previously found to have two H I absorption features with a total column density of $N_{\rm H\,I}=3.1\ 10^{20}\ {\rm cm}^{-2}$ (assuming a spin temperature of 100 K) (McNamara et al. 1990). Its central colors are consistent with a normal old population lacking recent star formation: a weak 4.6 Å equivalent width [O II]λ3727 nuclear emission line is present (McNamara & O'Connell 1989). The H I is infalling onto the central galaxy with velocities of $\sim$90–225 km s^{-1}; the absorption FWHM's are 62 and 35 km s^{-1}, respectively. The velocities of the absorption features and the central galaxy's systemic stellar velocity are indicated in Fig. 1. The location of the clouds is uncertain due to the large beam of the Arecibo telescope, and the presence of a continuum source located $\sim$1′ away from the nucleus. The JCMT beam was centered on the nucleus of NGC 5920. Therefore, we would not be sensitive to molecular gas located near the extranuclear continuum source. As is seen in Fig. 1 and indicated in Table 2, we obtained only an upper limit for the molecular gas content of $\lesssim 2\ 10^9 M_\odot$ near the nucleus. This is similar to the H I limit, $\lesssim 1.7\ 10^9 M_\odot$, found with the Arecibo observations.

The smallest H_2 limit ($\lesssim 4\ 10^8 M_\odot$) was found for NGC 3311, the centrally dominant galaxy in the A1060 cluster. This object has a weak blue central color anomaly, H II-region-like emission lines, and $\sim 3\ 10^4 M_\odot$ of dust in its central few kiloparsecs (Vasterberg et al. 1991; McNamara & O'Connell 1992). The weak central color

anomaly is consistent with a modest star-formation rate of ~ 0.1–$0.2 M_\odot$ yr^{-1}, assuming the Local initial mass function (IMF). This rate is only $\sim 10\%$ of $\dot{m}_{\rm CF}$. The H_2 upper limits, dust mass, and blue central colors are consistent with modest star formation and a gas-to-dust ratio that is similar to what is found in the Galaxy (cf. Young & Scoville 1991).

Unusually blue central colors have been found in Hydra A by Smith & Heckman (1989). Local fluxes and colors would be needed to estimate star formation rates, but are not presented there. However, the color anomaly in Hydra A is similar in size to those for the centrally dominant galaxies in A 1795 and A 2597, which have probable star formation rates between ~ 10–$40 M_\odot$ yr^{-1} (McNamara & O'Connell 1993). This assumes that all of the blue light is due to star formation, rather than nonthermal light from an active nucleus, and that the Local IMF applies. At these rates, the limits on the amount of molecular gas in Hydra A would be inconsistent with Local conditions. By comparison, a typical Sb–Sc galaxy has a star formation rate of $\sim 4 M_\odot$ yr^{-1} (Kennicutt 1983) and a molecular gas mass of $\sim 10^{10} M_\odot$ (e.g. Young & Scoville 1991). The gas depletion timescale implied for Hydra A is $\sim 10^{7-8}$ yr, 2–3 orders of magnitude shorter than disk galaxies, but consistent with "star-burst" galaxies.

Cygnus A, a well studied double-lobed radio elliptical galaxy (Perley et al. 1984), appears to be centered in a cooling flow (Arnaud 1988). It has strong nuclear emission lines, anomalously blue continuum light in its central regions, and central extinction attributable to dust (see Vestergaard & Barthel 1993 for a recent discussion). An earlier search for CO(1–0) with the NRAO 12 m telescope (Mirabel et al. 1989) resulted in upper limits similar to ours for CO(2–1).

NGC 1275 is the only example of a galaxy detected in CO which is centered in a cluster cooling flow. NGC 1275 also has blue central colors and a considerable amount of dust (cf. Rubin et al. 1977). However, far UV images indicate an absence of O stars (Smith et al. 1992). Their data are consistent with continuous star formation with a truncated (non-local) IMF, or the aging remains of continuous star formation that ended ~ 70 Myr ago with rates of ~ 15–$20 M_\odot$ yr^{-1}. The equivalent gas depletion timescale is $\sim 5\ 10^8$ yr, somewhat longer than the upper limits for the remaining objects, but perhaps consistent with a star-burst galaxy.

3.2. *Comparison to a cooling-flow model*

The X-ray surface brightness profiles of clusters appear to be consistent with distributed cooling (in the absence of heating) over a large range of radius. The radial dependence is not well determined, but is usually assumed to be $\dot{m} \propto R$ (cf. Thomas et al. 1987; White & Sarazin 1987) to the "cooling radius" (~ 150 kpc), where the cooling time reaches the assumed age of the cluster. (Table 1, Column 7). Our beam samples a small fraction of the total region inferred to be cooling, so we may not be sensitive to the total cooling mass.

Assuming $\dot{m} \propto R$, the cooling rate per year within our 21″ beam is: $\dot{M}(d) \sim \dot{m}_{\rm CF}(\pi/2)(R_{\rm beam}/R_{\rm cool})$, where $R_{\rm beam}$ is half the beam diameter in Table 2, and $\dot{m}_{\rm CF}$ and $R_{\rm cool}$ are the total mass accretion rate integrated over all radii, and the cooling radius respectively, in Table 1. The geometrical factor is a correction for cooling at large radii projected onto the beam. The estimated cooling rates within the telescope beam are given in Table 1.

The off-beam position was within $R_{\rm cool}$ for most clusters. Cold gas present at these radii could, in principle, cancel a signal at the central beam position. This is unlikely unless the radial cooling function is steeper than we have assumed. Standard cooling flow models predict a surface density of cooling material which decreases with radius. The contribution from the off position should be only $\sim 15\%$ of the central position; the off position was outside the cooling region of Hydra A and Cygnus A. In addition, warm and cold gas is generally observed within about $0.1 R_{\rm cool}$. Therefore, significant contamination of our off-beam by cooling material seems unlikely and will be ignored.

The $I_{\rm CO}$ estimates (cf. Sect. 2.3; Table 2) correspond to clouds with velocity spreads similar to those observed in NGC 1275. These values would increase for larger angular sizes and velocity spreads. The conversion to $M_{\rm H_2}$ is relevant to Galactic-like clouds. We use limits on the amount of molecular material with these properties deposited within the beam by the cooling flow as an "accumulation" timescale defined as $t_{\rm a} \lesssim M_{\rm H_2}/\dot{m}_{\rm CF}(d)$. These values, Table 2 Column 9, usually imply the presence of $\lesssim 10^8$ yr worth of accumulated molecular material, and $\lesssim 4\ 10^7$ yr worth in the largest accretor Hydra A. Similar mass limits and accumulation timescales are found using H I (McNamara et al. 1990). These timescales would be $5\times$–$10\times$ shorter for preferential cooling in the central regions. The molecular material observed in NGC 1275 (corrected for beam size) corresponds to $\sim 6\ 10^8$ yr worth of accumulated material, somewhat larger than the limits for this sample but $\sim 15\times$ larger than found for Hydra A.

These observations are not consistent with a molecular state for cooling material from a steady-state 10 Gyr old cooling flow, unless cold clouds are accelerated to large velocity dispersions on short timescales ($\lesssim 10^8$ yr), or they differ considerably from Galactic clouds. The limits are probably consistent with a non gaseous (i.e. stellar or planetary debris) repository. The accumulation timescales are, however, close to collapse timescales for Jeans unstable clouds at cooling flow pressures ($\sim 5\ 10^7$ yr; Bregman et al. 1988). The product of the collapse time and $\dot{m}_{\rm CF}$ should be roughly the minimum mass of cold gas present if the cooling material is converted into a non-gaseous state. CO and H I upper limits significantly lower than these would be problematic for simple cooling-flow models.

3.3. *Limits on cloud populations*

Our $\sim 600\ \mathrm{km\ s^{-1}}$ bandwidth limits the sensitivity to molecular gas with a high velocity dispersion. A cloud population with large velocity dispersion and mass $\gtrsim 10^{11} M_\odot$ has been proposed as the origin of anomalies found in soft X-ray spectra of clusters (e.g. White et al. 1991; Mushotzky 1992; Daines et al. 1993). Such a population could be the repository for the cooling gas, or residual gas from cluster formation. If the final state of the putatively cooling ICM is primarily molecular gas, the steady state cooling flow models predict that $\sim 10^{11} M_\odot$ of molecular material should be present in our beam. Using simple model spectra, we estimate the properties these clouds must have to avoid detection.

Our model CO(2–1) spectra are anchored to the CO(2–1) and CO(1–0) emission line properties of NGC 1275 (Lazareff et al. 1989). We assumed that the integrated brightness temperatures of NGC 1275's CO emission features correspond to a molecular mass of $10^{10} M_\odot$ (for $H_o = 50\ \mathrm{km\ s^{-1}\ Mpc^{-1}}$). We adopted the observed ratio of the integrated brightness temperatures in the CO(1–0) and CO(2–1) features [CO(1–0)/CO(2–1)= 1.67] when converting our model features to molecular gas mass. The model spectra were constructed by creating a zero level baseline with a velocity width and random noise spectrum identical to the observed spectra, after linear baseline subtraction. A Gaussian-shaped CO emission feature was added to the noisy baseline. The amplitude and σ of the model feature were varied to simulate populations with different masses and velocity dispersions. The integrated brightness temperature was assumed to increase proportionally to the mass of the cloud population. A test model for MKW 3s was constructed by adding a Gaussian feature with identical σ to the feature in NGC 1275, and an amplitude scaled by the ratio of the square of their redshifts. The model feature's area was measured, and a mass was computed similarly to the method used with the real spectra. This procedure returned the input mass to $\sim 20\%$, so the model is self consistent. The molecular mass estimate for NGC 1275 applies to material with similar physical and chemical properties to clouds in the Galaxy and nearby spirals. Departures from this assumption will directly affect our mass scale. Whereas NGC 1275's unusual properties render it less than ideal for comparison, it is the only cooling flow cluster yet detected in CO.

Our models show that a massive, high velocity dispersion cloud population can cause detectable spectral distortions and brightness temperature increases. In Figs. 2 and 3 we show the models of MKW 3s and Hydra A, assuming a range of molecular gas masses and population velocity dispersions. The scales of Figs. 2 and 3 are identical to those of Fig. 1. Panel A in Figs. 2 and 3 shows an equivalent CO(2–1) feature for NGC 1275 but appropriately scaled for distance. These model spectra show significant baseline curvature and brightness temperature increases. Similar features in our program spectra, if present, would have been easily detected.

The remaining panels show the model spectra for a total cloud mass of $\sim 10^{11} M_\odot$ and population velocity dispersions ranging from 300–1000 $\mathrm{km\ s^{-1}}$. The masses would correspond roughly to the total accumulated material in our beam for a cooling-flow age of $\sim 10^{10}$ yr. The velocities range from typical cD galaxy velocity dispersions to cluster dispersions (Malumuth & Kirshner 1985; Zabludoff et al. 1990). The model spectra show significant curvature for velocity dispersions $\sigma \lesssim 500\ \mathrm{km\ s^{-1}}$ and increases in the baseline brightness temperatures. A comparison to the MKW 3s spectrum shows that a cloud population with a mass of $\sim 10^{11} M_\odot$ and $\sigma \lesssim 500\ \mathrm{km\ s^{-1}}$ would have been detected as a significant baseline curvature and a brightness temperature anomaly. For $\sigma \sim 1000\ \mathrm{km\ s^{-1}}$, there would be no detectable baseline curvature, but perhaps a detectable increase in the brightness temperature. We can exclude a $10^{11} M_\odot$ cloud population with $\sigma \lesssim 500\ \mathrm{km\ s^{-1}}$ in Hydra A. The most sensitive limit was found for the nearby cluster A 1060. Limits on its continuum temperature exclude a population with a mass $\gtrsim 10^9 M_\odot$ at all velocities considered here, although a weak emission feature near the stellar velocity of NGC 3311 may be present in its spectrum. The presence of a $10^{11} M_\odot$ cloud population is excluded at all velocities in A 2256, but a $\sim 10^{10} M_\odot$ population with a velocity dispersion exceeding $\sim 100\ \mathrm{km\ s^{-1}}$ is consistent with the data. We exclude a population of clouds in A 2151 with a mass of $10^{11} M_\odot$ and $\sigma \lesssim 1000\ \mathrm{km\ s^{-1}}$, but a $10^{10} M_\odot$ population with $\sigma \gtrsim 300\ \mathrm{km\ s^{-1}}$ is not excluded. Finally, due to its significant continuum level, Cygnus A could have molecular material present well in excess of $10^{11} M_\odot$, provided it has a velocity dispersion ($\gtrsim 500\ \mathrm{km\ s^{-1}}$). However, it is likely that much of its continuum is due to the central radio source, rather than molecular gas. This could be true of the remaining objects, which would imply a conservative interpretation of these limits.

The large column densities of absorbing material inferred to be present in cooling flows from their *Einstein* Observatory Solid State Spectra (White et al. 1992) are difficult to reconcile with H I observations (e.g. McNamara et al. 1990). To avoid discrepancy, White et al. have suggested that the absorbing material is opaque, very cold (~ 10 K) clouds with covering factors near unity. Emission from an ensemble of optically thick clouds which fill the telescope beam would have been detected, unless they are colder than $T_c \sim 10$ K and have a velocity dispersion $\sigma \gtrsim 500\ \mathrm{km\ s^{-1}}$. The peak antenna temperature of a population of clouds with temperatures T_c and an ensemble velocity dispersion σ is $T_a \sim 4[T_c^{3/2}(10\ \mathrm{K})/\sigma_{500}]$ mK. The signal would be roughly Gaussian in shape. Based on the continuum temperatures (Table 2, Column 3), and the absence of significant spectral distortions (cf. Fig. 1), this is probably excluded in half of the sample, unless the clouds have significantly larger velocity dispersions.

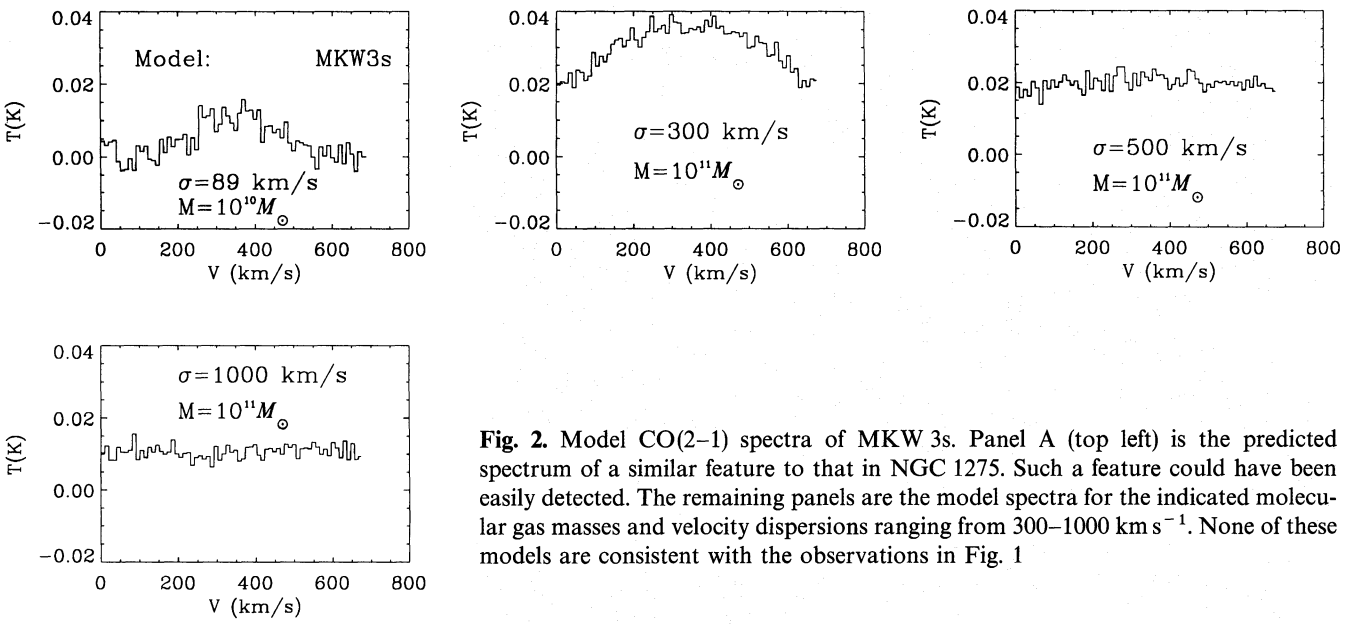

Fig. 2. Model CO(2–1) spectra of MKW 3s. Panel A (top left) is the predicted spectrum of a similar feature to that in NGC 1275. Such a feature could have been easily detected. The remaining panels are the model spectra for the indicated molecular gas masses and velocity dispersions ranging from 300–1000 km s^{-1}. None of these models are consistent with the observations in Fig. 1

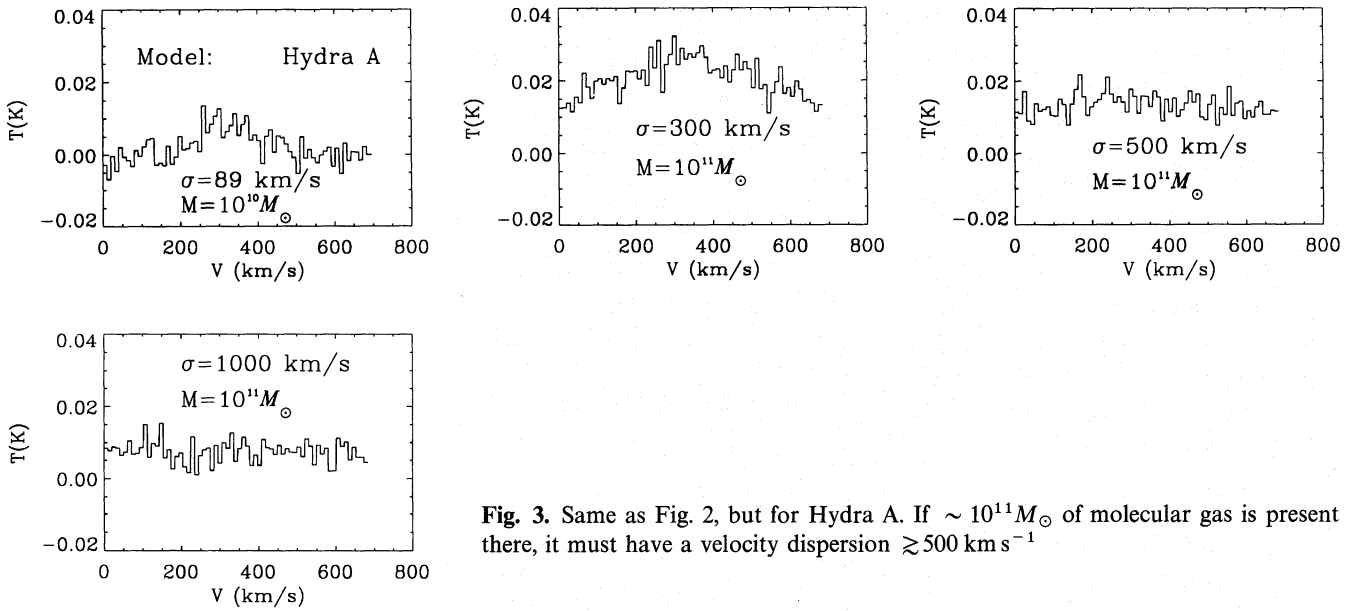

Fig. 3. Same as Fig. 2, but for Hydra A. If $\sim 10^{11} M_{\odot}$ of molecular gas is present there, it must have a velocity dispersion $\gtrsim 500$ km s^{-1}

In the aggregate, our results do not support the accumulation molecular material with velocity dispersions similar to other tracers of cool gas (i.e. Hα, & H I). If the cooling rates derived from X-ray observations are correct, a non-gaseous or stellar repository is likely. As discussed above, our limits are also straining this possibility. Short accumulation timescales may be avoided by appealing to younger cooling-flow ages (c.f. Hu 1988). Our constraints, however, refer to the total amounts of molecular material present in our beam. Substantial amounts of molecular material distributed throughout the cooling region could avoid detection, although a higher surface density of material at larger radii would be inconsistent with current steady-state cooling flow models.

Massive cloud populations colder and metal deficient with respect to clouds in the Galaxy and nearby spirals could have avoided detection. The conversion from CO brightness temperature to molecular gas mass relies heavily on local observations which generally apply to clouds at temperatures of $T \sim 10$–15 K with solar chemical composition (Sanders et al. 1984). Assuming the integrated brightness temperature is proportional to the cloud temperatures, the mass limits could be increased by factors of 3–5 for cloud temperatures $\gtrsim 3$ K. It is not clear whether it is plausible to maintain molecular material at these temperatures over cluster ages. Cluster halo metallicities are usually close to or just below solar (Mushotzky & Szymkowiak 1988), so

an anomalous metallicity is unlikely to introduce a substantial error.

3.4. Summary

We presented sensitive CO(2–1) spectra, obtained with the 15 m James Clerk Maxwell Telescope, of the central $\sim$25 kpc of six cluster cooling flows. CO was not detected either in emission or absorption. We discussed the following results:

(1) Our limits on the molecular gas mass in the inner $\sim$25 kpc, integrated over velocities $\lesssim 300\,\mathrm{km\,s^{-1}}$, are estimated to be typically $M_{\mathrm{H_2}} \lesssim 4\,10^9\,M_\odot$. This limit is $M_{\mathrm{H_2}} \lesssim 4\,10^8 M_\odot$ for A 1060.

(2) Molecular gas with similar properties to that in NGC 1275, if present, would have been detected in all of our objects.

(3) Using model spectra, we exclude cloud populations with masses much greater than a few $10^{10} M_\odot$ and velocity dispersions $\lesssim 500\,\mathrm{km\,s^{-1}}$. A cloud population with a velocity dispersion $\gtrsim 1000\,\mathrm{km\,s^{-1}}$ and a mass $\gtrsim 10^9 M_\odot$ is excluded in the nearby cluster A 1060. These limits could be relaxed if molecular gas is present at a temperature well below Galactic molecular cloud temperatures, or has an unusually low metal abundance.

(4) If the steady state cooling flow model is to avoid being inconsistent with the observations, the cooling material must be efficiently converted to a non gaseous state on a timescale of $\sim 10^{7-8}$ yr, or cold clouds must be accelerated to high velocity dispersion ($\gtrsim 700\,\mathrm{km\,s^{-1}}$) on a similar timescale. Similar conclusions have been reached using earlier H I observations. Improved measurements with broader bandwidths may result in more stringent limits. Limits significantly lower than these may be hard to reconcile with simple, steady state cooling flow models.

Acknowledgements. We thank Thijs van der Hulst for stimulating this project in its early stages and for his comments on the manuscript.

References

Arnaud K.A., 1988 (unpublished)
Baum S.A., Heckman T., Bridle A., van Breugel W., Miley G., 1988, ApJS 68, 643
Bothun G.D., Schombert J.M., 1990, ApJ 360, 436
Bregman J.N., Hogg, 1988, AJ 96, 455
Burns J.O., White R.A., Haynes M.P., 1981, AJ 86, 1120
Daines S.J., Fabian A.C., Thomas P.A., 1993 (in preparation)
David L.P., Arnaud K.A., Forman W., Jones C., 1990, ApJ 356, 32
Dressler A., Shectman S., 1988, AJ 95, 284
Fabian A.C., 1988, Cooling Flows in Clusters and Galaxies. Kluwer, Dordrecht
Fabian A.C., 1992, Clusters and Superclusters of Galaxies. Kluwer, Dordrecht
Fabricant D.G., Kent S.M., Kurtz M.J., 1989, ApJ 336, 77
Forman W., Jones C., 1982, ARA&A 20, 547
Grabelski D.A., Ulmer M.P., 1990, 355, 401
Hu E.M., 1988, in: Fabian A.C. (ed.) Cooling Flows in Clusters of Galaxies. Dordrecht, Kluwer, p. 73
Jaffe W., 1990, AA 240, 254
Jaffe W., 1992, in: Fabian A.C. (ed.) Clusters and Superclusters of Galaxies. Kluwer, Dordrecht
Kennicutt R.C., 1983, ApJ 272, 54
Lazareff B., Castets A., Kim D.W., Jura M., 1989, ApJ 336, L13
Malumuth E.M., Kirshner R.P., 1985, ApJ 291, 8
McNamara B.R., Bregman J.N., O'Connell R.W., 1990, ApJ 360, 20
McNamara B.R., O'Connell R.W., 1989, AJ 98, 2018
McNamara B.R., O'Connell R.W., 1992, ApJ 393, 579
McNamara B.R., O'Connell R.W., 1993, AJ 105, 417
Mirabel I.F., Sanders D.B., Kazes I., 1989, ApJ 340, L9
Mushotzky R.F., Szymkowiak A.E., 1988, in: Fabian A.C. (ed.) Cooling Flows in Clusters of Galaxies. Kluwer, Dordrecht, p. 53
Mushotzky R.F., 1992, in: Fabian A.C. (ed.) Clusters and Superclusters of Galaxies. Kluwer, Dordrecht
O'Dea C.P., Baum S.A., Maloney P.R., Tacconi L.J., Sparks W.B., 1993, ApJ (submitted)
Osterbrock D.E., Miller J.S., 1975, ApJ 197, 535
Perley R.A., Dreher J.W., Cowan J.J., 1984, ApJ 285, L35
Rubin V.C., Ford W.K. Jr., Peterson C.J., Oort J.H., 1977, ApJ 211, 693
Sarazin C.L., 1986, Rev. Mod. Phys. 58, 1
Sanders D.B., Solomon P.M., Scoville N.Z., 1984, ApJ 276, 182
Simkin S.M., 1979, ApJ 234, 56
Smith E.P., Heckman T.M., 1989, ApJS 69, 365
Smith E.P., O'Connell R.W., Bohlin R.C., Kwang-Ping Cheng Cornette R.H., Hill J.K., Hill R.S., Hintzen P., Landsman W.B., Neff S.G., Roberts M.S., Smith A.M., Stecher T.P., 1992, ApJ 395, L49
Thomas P.A., Fabian A.C., Nulsen P.E.J., 1987, MNRAS 228, 973
Valentijn E.A., Giovanelli R., 1982, A&A 114, 208
Vasterberg A.R., Jorsater S., Lindblad P.O., 1991, A&A 247, 335
Vestergaard M., Barthel P.D., 1993, AJ 105
White D.A., Fabian A.C., Johnstone R.M., Mushotzky R.F., Arnaud K.A., 1991, MNRAS 252, 72
White R.E. III, Sarazin C.L., 1987, ApJ 318, 612
White R.E. III, Sarazin C.L., 1988, ApJ 335, 688
Young J.S., Scoville N.Z., 1991, ARAA 29, 581
Zabludoff A.I., Huchra J.P., Geller M.J., 1990, ApJS 74, 1

Note added in proof: Following acceptance of this paper, we received a copy of a paper similar to this one by O'Dea et al. (1993), which has been submitted to the Astrophysical Journal. Their limits in CO1→0 for 3 cooling flow clusters are similar to ours, as are their conclusions.